Langmuir Article

pubs.acs.org/Langmuir

Homochiral Recognition among Organic Molecules on Copper(110)

Huanyao Cun,[†] Yeliang Wang,[†] Bing Yang,[†] Lei Zhang,[†] Shixuan Du,[†] Yue Wang,[‡] Karl-Heinz Ernst,*[,§] and Hong-Jun Gao*[,†]

[†]*Institute of Physics, Chinese Academy of Sciences, Beijing 100190, China,* [‡]*Key Lab of Supramolecular Structure and Materials, Jilin University, Changchun 130023, China, and* [§]*Empa, Swiss Federal Laboratories for Materials Testing and Research, Uberlandstrasse 129, CH-8600 Dübendorf, Switzerland*

Received August 26, 2009. Revised Manuscript Received September 30, 2009

The adsorption of a prochiral quinacridone derivative (QA16C) with two alkyl chains of 16 carbon atoms on a Cu(110) surface was investigated with variable-temperature scanning tunneling microscopy. QA16C molecules prefer to assemble at 150 K into short homochiral molecular lines with two enantiomorphous orientations in which the lateral alkyl chains exhibit partial disorder. With increasing sample temperatures, the QA16C lines form larger well-ordered homochiral domains. As a reason for the homochiral recognition, we identify a rigid alignment of the molecule due to the interaction with the substrate. In addition, lateral intermolecular interactions in the form of hydrogen bonding and van der Waals interactions are identified.

Introduction

Molecular recognition of chiral molecules on surfaces plays an important role in processes such as enantiomeric separation of chiral compounds,[1] crystal growth,[2−5] enantiospecific sensors,[6,7] and heterogeneous asymmetric catalysis.[8,9] Despite its importance, the mechanism of chiral recognition in these surface processes is poorly understood.[10] Ever since Pasteur's separation of enantiomorphous ammonium sodium tartrate crystals and his realization that there is a connection between crystal enantiomorphism and the handedness of the molecular building blocks, there has been a growing interest in understanding the mechanisms of chiral resolution during crystallization at the molecular level. However, there are still no satisfying explanations for the fact that some chiral compounds undergo optical resolution but the vast majority do not.[11] Moreover, the transfer of chirality into mesoscopic structures, a very important issue in liquid crystal science, is difficult to predict. Because of the complex situation, well-defined model systems are a good approach to gaining insight into these processes at a molecular level. This has been demonstrated in the field of heterogeneous catalysis, where details of surface reactions have been investigated on single-crystal surfaces in ultrahigh vacuum (UHV), i.e., far from the working conditions.[12] Therefore, the adsorption of chiral molecules on single-crystal surfaces is increasingly deployed as an approach for better understanding the phenomenon of optical resolution of enantiomers.[13] In particular, the possibility of studying these processes with submolecular resolution in these two-dimensional (2D) systems by using scanning tunneling microscopy (STM) has substantially increased the number of chiral surface science studies over the past decade.[14]

It has been predicted that 2D chiral resolution on a surface should occur more easily than in three-dimensional crystals.[15] Due to confinement in the plane, certain symmetry elements, like the center of inversion or the glide plane parallel to the surface, are precluded, and enhanced chiral interactions are therefore expected.[16] However, the balance between the molecule−substrate interaction and the lateral intermolecular interactions determines the nature of self-assembly[17] and thus the outcome of lateral resolution. Different enantiomorphous surface structures, including mirror domains,[18−20] clusters,[21−23] and filaments,[24] as well as chiral phenomena, like enantiospecific recognition,[25] chiral switching,[26] and chiral amplification,[27−31] have been reported. Here we show that the alignment of the molecule on the surface

*To whom correspondence should be addressed. E-mail: hjgao@aphy.iphy.ac.cn or karl-heinz.ernst@empa.ch.

(1) Pirkle, W. H.; Reno, D. S. *J. Am. Chem. Soc.* **1987**, *109*, 7189.
(2) Vaida, M.; Shimon, L. J.; van Mil, J.; Ernst-Cabrera, K.; Addadi, L.; Leiserowitz, L.; Lahav, M. *J. Am. Chem. Soc.* **1989**, *111*, 1029.
(3) Weissbuch, I.; Addadi, L.; Lahav, M.; Leiserowitz, L. *Science* **1991**, *253*, 637.
(4) Hazen, R. M.; Filley, T. R.; Goodfriend, G. A. *Proc. Natl. Acad. Sci. U.S.A.* **2001**, *98*, 5487.
(5) Orme, C. A.; Noy, A.; Wierzbicki, A.; Bride, M. T.; Grantham, M.; Teng, H. H.; Dove, P. M.; DeYoreo, J. J. *Nature* **2001**, *411*, 775.
(6) Bodenhöfer, K.; Hierlemann, A.; Seeman, J.; Gauglitz, G.; Koppenhöfer, B.; Göpel, W. *Nature* **1997**, *387*, 577.
(7) McKendry, R.; Theoclitou, M.-E.; Rayment, T.; Abell, C. *Nature* **1998**, *391*, 566.
(8) Izumi, Y. *Adv. Catal.* **1983**, *32*, 215.
(9) Baiker, A. *J. Mol. Catal. A: Chem.* **1997**, *115*, 473.
(10) Raval, R. *Nature* **2003**, *425*, 463.
(11) Pérez-García, L.; Amabilino, D. B. *Chem. Soc. Rev.* **2007**, *36*, 941.
(12) Ertl, G. *Angew. Chem., Int. Ed.* **2008**, *47*, 3524.
(13) Ernst, K.-H. *Top. Curr. Chem.* **2006**, *265*, 209.
(14) Raval, R. *Chem. Soc. Rev.* **2009**, *38*, 707.
(15) Arnett, E. M.; Chao, J.; Kinzig, B.; Stewart, M. V.; Thompson, O.; Verbiar, R. J. *J. Am. Chem. Soc.* **1982**, *104*, 389.
(16) Lahav, M.; Leiserowitz, L. *Angew. Chem., Int. Ed.* **1999**, *38*, 2533.
(17) Barlow, S. M.; Louafi, S.; Le Roux, D.; Williams, J.; Muryn, C.; Haq, S.; Raval, R. *Langmuir* **2004**, *20*, 7171.
(18) Wei, Y. H.; Kannappan, K.; Flynn, G. W.; Zimmt, M. B. *J. Am. Chem. Soc.* **2004**, *126*, 5318.
(19) Fasel, R.; Parschau, M.; Ernst, K. H. *Angew. Chem., Int. Ed.* **2003**, *42*, 5178.
(20) Cai, Y.; Bernasek, S. L. *J. Phys. Chem. B* **2005**, *109*, 4514.
(21) Böhringer, M.; Morgenstern, K.; Schneider, W.-D.; Berndt, R.; Mauri, F.; Vita, A. D.; Car, R. *Phys. Rev. Lett.* **1999**, *83*, 324.
(22) Blüm, M. C.; Cavar, E.; Pivetta, M.; Patthey, F.; Schneider, W. D. *Angew. Chem., Int. Ed.* **2005**, *44*, 5334.
(23) Kühnle, A.; Linderoth, T. R.; Besenbacher, F. *J. Am. Chem. Soc.* **2003**, *125*, 14680.
(24) Barth, J. V.; Weckesser, J.; Trimarchi, G.; Vladimirova, M.; Vita, A. D.; Cai, C.; Brune, H.; Günter, P.; Kern, K. *J. Am. Chem. Soc.* **2002**, *124*, 7991.
(25) Rao, B. V.; Kwon, K. Y.; Zhang, J.; Liu, A. W.; Bartels, L. *Langmuir* **2004**, *20*, 4406.
(26) Weigelt, S.; Busse, C.; Petersen, L.; Rauls, E.; Hammer, B.; Gothelf, K. V.; Besenbacher, F.; Linderoth, T. R. *Nat. Mater.* **2006**, *5*, 112.
(27) Fasel, R.; Parschau, M.; Ernst, K. H. *Nature* **2006**, *439*, 449.
(28) Parschau, M.; Romer, S.; Ernst, K.-H. *J. Am. Chem. Soc.* **2004**, *126*, 15398.
(29) Parschau, M.; Kampen, T.; Ernst, K.-H. *Chem. Phys. Lett.* **2005**, *407*, 433.
(30) Parschau, M.; Fasel, R.; Ernst, K.-H. *Cryst. Growth Des.* **2008**, *8*, 1890.
(31) Haq, S.; Liu, N.; Humblot, V.; Jansen, A. P. J.; Raval, R. *Nat. Chem.* **2009**, *1*, 409.

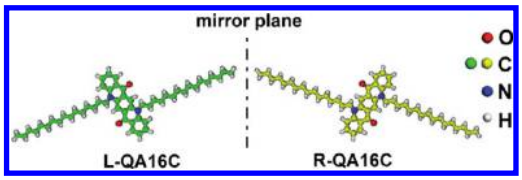

Figure 1. Molecular structure of QA16C enantiomers at the surface. The molecule consists of an aromatic quinacridone backbone and two alkyl chains with 16 carbon atoms.

can be decisive regarding optical resolution. Because of a strict adsorption mode, only lateral homochiral interactions are observed. No matter the coverage or the temperature, homochiral recognition prevails over heterochiral intermolecular interactions.

As a model system, we chose *N*,*N*′-dihexadecylquinacridone [$C_{52}H_{76}O_2N_2$, QA16C (Figure 1)] on Cu(110) under UHV conditions. Quinacridone and its derivatives are well-known organic semiconductor materials, which display excellent chemical stability[32] and are promising candidates for high-performance organic light-emitting devices.[33] QA16C has two alkyl chains with 16 carbon atoms each and an aromatic backbone. The molecules are achiral in the gas or liquid phase but become chiral upon adsorption. Therefore, QA16C molecules are distinguishable on the surface as left- and right-handed enantiomers [L- and R-QA16C, respectively (Figure 1)]. Moreover, the combination of rigid backbone and flexible alkyl side chains also makes QA16C an interesting model for understanding the intermolecular interactions in liquid crystal science. We have shown previously that the self-assembly behavior of *N*,*N*′-dialkyl-substituted quinacridone derivatives on a Ag(110) surface is clearly modulated by the length of the lateral alkyl chains.[34] Several STM investigations of QA self-assembly have also been conducted at the solid−liquid interface on highly oriented pyrolytic graphite (HOPG).[35−41] For example, De Feyter et al. found that all QA and QA analogue molecular alkyl chains are interdigitated.[39,40] Despite the orientation of the alkyl chains along the ⟨1100⟩ surface azimuthal directions of HOPG, they suggested that formation of these structures was basically driven by intermolecular interactions. Liquid−solid interface studies on HOPG have disadvantages in that the temperature range is very narrow (usually room temperature only) and that the molecules are too mobile to be imaged at coverages below the saturated monolayer. Our study, on the other hand, demonstrates that molecular recognition at initial stages of self-assembly can be studied with long alkyl side chain molecules at different coverages and over a broader temperature range under UHV conditions.

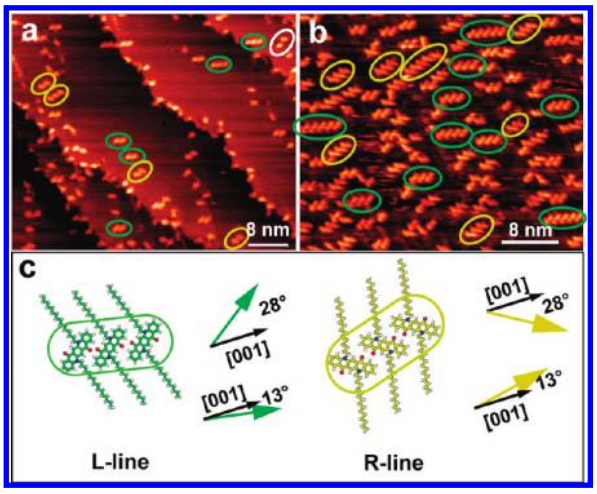

Figure 2. (a and b) STM images obtained at 150 K on Cu(110) at low QA16C coverages. One-dimensional structures of QA16C with different orientations are observed. Monomers, dimers, trimers, tetramers, and pentamers are identified. (c) Schematic representation of backbone and line orientations. (a) $U_{bias} = -1.07$ V, and $I_t = 0.50$ nA. (b) $U_{bias} = -1.29$ V, and $I_t = 0.08$ nA.

Experimental Section

The experiments were performed in an ultrahigh vacuum (UHV) system with a base pressure of 1.0×10^{-10} mbar. The system was equipped with a variable-temperature scanning tunneling microscope (VT-STM, Omicron Nanotechnology) and evaporation sources.[42,43] The single-crystal Cu(110) (orientation accuracy of $< 0.1°$, MaTeck GmbH) has been prepared in vacuo as described previously.[44,45] QA16C was purified by sublimation at 10^{-7} mbar, followed by degassing at 440 K for several hours under UHV conditions, which removed more volatile impurities sufficiently. The Cu(110) substrate was cooled to 135 K prior to deposition. QA16C was sublimed from an evaporation cell held at 460 K. The STM measurements were taken with an electrochemically etched tungsten tip at sample temperatures ranging from 150 to 300 K. All STM images were taken in constant-current mode with negative and positive voltages. Since the quality of STM images obtained with negative biases was higher, we present only images acquired with negative biases.

Results and Discussion

Panels a and b of Figure 2 display large-scale STM images of QA16C on Cu(110) at 150 K with coverages of ∼0.3 and ∼0.5 monolayer (ML), respectively. One ML is here defined as the closed-packed monolayer of QA16C (as presented further below), i.e., one molecule per 33 Cu(110) surface atoms or 3.05 nm^2, also corresponding to ∼0.33 molecule/nm^2. The QA16C backbones are well-resolved in STM images for single molecules, but the alkyl chains are not observed. At 0.3 ML, the QA16C molecules are dispersed as monomers, dimers, trimers, and tetramers in short linear structures. The majority of the molecules are found in dimers. At somewhat higher coverage (0.5 ML), the QA16C molecules still form these lines with a higher abundance of tetramer and pentamer units. No islands are observed at 150 K at these low coverages, which implies that the intermolecular interactions are highly directional among the molecules at this

(32) Wang, J.; Zhao, Y.; Zhang, J.; Zhang, J.; Yang, B.; Wang, Y.; Zhang, D.; You, H.; Ma, D. *J. Phys. Chem. C* **2007**, *111*, 9177.
(33) Gross, E. M.; Anderson, J. D.; Slaterbeck, A. F.; Thayumanavan, S.; Barlow, S.; Zhang, Y.; Marder, S. R.; Hall, H. K.; Nabor, M. F.; Wang, J. F.; Mash, E. A.; Armstrong, N. R.; Wightman, R. M. *J. Am. Chem. Soc.* **2000**, *122*, 4972.
(34) Shi, D.; Ji, W.; Lin, X.; He, X.; Lian, J.; Gao, L.; Cai, J.; Lin, H.; Du, S.; Lin, F.; Seidel, C.; Chi, L.; Hofer, W.; Fuchs, H.; Gao, H. J. *Phys. Rev. Lett.* **2006**, *96*, 226101.
(35) Ye, K.; Wang, J.; Sun, H.; Liu, Y.; Mu, Z.; Li, F.; Jiang, S.; Zhang, J.; Zhang, H.; Wang, Y.; Che, C.-M. *J. Phys. Chem. B* **2005**, *109*, 8008.
(36) Qiu, D. L.; Ye, K. Q.; Wang, Y.; Zou, B.; Zhang, X. *Langmuir* **2003**, *19*, 678.
(37) Giancarlo, L. C.; Flynn, G. W. *Acc. Chem. Res.* **2000**, *33*, 491.
(38) Tao, F.; Bernasek, S. L. *J. Am. Chem. Soc.* **2005**, *127*, 12750.
(39) Keller, U.; Müllen, K.; DeFeyter, S.; DeSchryver, F. C. *Adv. Mater.* **1996**, *8*, 490.
(40) De Feyter, S.; Gesquiere, A.; De Schryver, F. C.; Keller, U.; Müllen, K. *Chem. Mater.* **2002**, *14*, 989.
(41) Yang, X. Y.; Wang, J.; Zhang, X.; Wang, Z.; Wang, Y. *Langmuir* **2007**, *23*, 1287.
(42) Wang, Y.; Gao, H.-J.; Guo, H.; Wang, S.; Pantelides, S. T. *Phys. Rev. Lett.* **2005**, *94*, 106101.
(43) Wang, Y.; Gao, H.-J.; Guo, H.; Liu, H. *Phys. Rev. B* **2004**, *70*, 073312.
(44) Ernst, K.-H.; Schlatterbeck, D.; Christmann, K. *Phys. Chem. Chem. Phys.* **1999**, *1*, 4105.
(45) Deng, Z.; Lin, H.; Ji, W.; Gao, L.; Lin, X.; Cheng, Z.; He, X.; Lu, J.; Shi, D.; Hofer, W. A.; Gao, H.-J. *Phys. Rev. Lett.* **2006**, *94*, 156102.

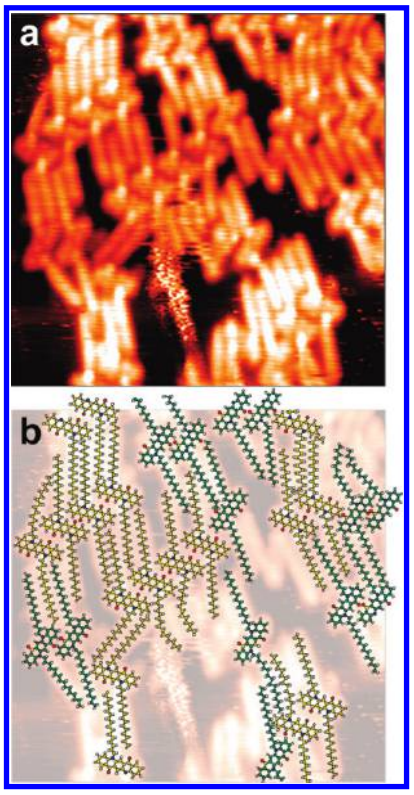

Figure 3. (a) Close-up STM image obtained at a sample temperature of 150 K and $\theta \approx 0.7$ ML. The backbones and the alkyl chains of the QA16C molecules are resolved. $U_{bias} = -1.50$ V, and $I_t = 0.10$ nA. (b) Overlay of the STM pattern shown in panel a and a drawing of molecular models. The carbon atoms of the R-enantiomers are colored yellow and those of the L-enantiomers green. Multiple orientations of the alkyl chains are found.

temperature. The QA16C backbones of single molecules adsorbed on the flat Cu(110) terraces align with only two specific orientations. Both are enantiomorphous with respect to the [001] direction of Cu(110). This means that the angle between the L-QA16C backbone and the [001] direction of the substrate is 28° and −28° for the R-QA16C backbone (Figure 2c). The backbone alignment in the oligomers is identical to that in the monomers. From this follows unambiguously that the corresponding molecular lines, regardless of their lengths, also have only two alignment directions. These two line modes are encircled by green and yellow lines in Figure 2. The angle for the L-line (green) is tilted by −13° clockwise with respect to the Cu [001] direction, while the angle for the R-line (yellow) is tilted by 13° counterclockwise. The intermolecular interactions therefore have no influence on the molecular orientation.

A distinct feature of the molecular lines is their homochirality. That is, the L-lines consist only of L-QA16C and R-lines only of R-QA16C molecules. All molecules in a single line are oriented parallel to each other. At this initial nucleation stage, lateral separation of the enantiomers already occurs, and the self-assembly of QA16C on Cu(110) proceeds enantioselectively. Mixed lines are not observed, because opposite-handed molecules cannot be arranged so closely together because of the different tilt angles. Heterochiral intermolecular interactions are therefore expected to be much weaker. An example of the closest observed heterochiral pair is marked with a white ellipse in Figure 2a. However, such pairs are rarely found. Homochiral line motifs on

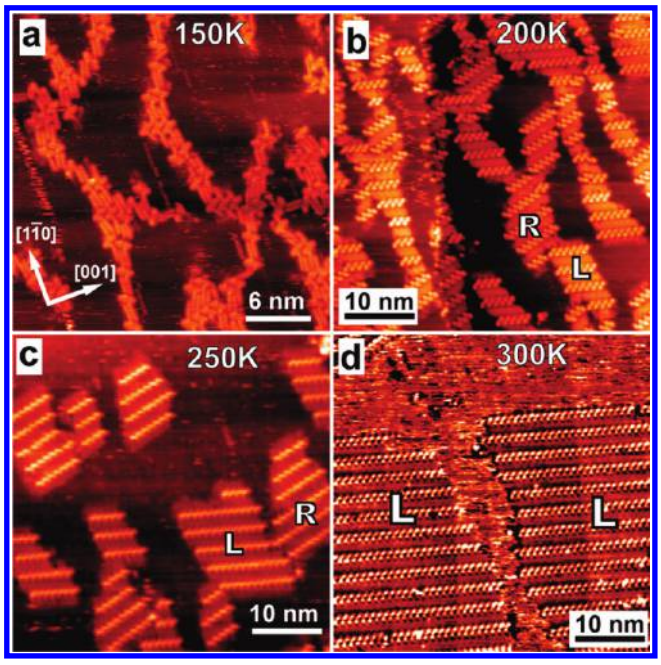

Figure 4. STM images showing the self-assembled QA16C patterns with increasing temperatures ($\theta \approx 0.7$ ML). (a) At 150 K, $U_{bias} = -1.26$ V and $I_t = 0.10$ nA. (b) At 200 K, $U_{bias} = -1.54$ V and $I_t = 0.20$ nA. (c) At 250 K, $U_{bias} = -1.26$ V and $I_t = 0.50$ nA. (d) At 300 K, $U_{bias} = -1.07$ V and $I_t = 0.80$ nA.

Cu(110) have been observed also for di-D-phenylalanine[46] and the prochiral adenine.[47] In both cases, directed lateral intermolecular hydrogen-bonded interactions have been proposed as enantioselector via theoretical calculations.

Figure 3a shows the situation at 150 K with further increased coverage in a close-up image of an aggregated pattern. Both the backbones and the lateral alkyl chains of QA16C molecules are well-resolved. The STM image is reproduced schematically in Figure 3b. Because of the steric interaction among adjacent molecules, multiple orientations of the alkyl chains are observed, while the backbones are still in their specific alignment. Hence, the angle between the alkyl chains and the respective backbone varies over a large range. This clearly indicates that the alkyl chains of QA16C molecules are relatively flexible and could explain why they are not resolved at low coverages. Compared to the backbone−substrate interactions, the alkyl chain interactions with the substrate are much weaker. At higher coverages, they become more confined because of steric interactions with neighboring molecules but still vary in their orientation. Nevertheless, a tendency to a more parallel alignment of the alkyl chains of the adjacent adsorbates can be observed.

Lateral ordering into the most stable configurations requires sufficient mobility of the components, which can to a certain extent be induced by increasing the sample temperature. Figure 4 shows a series of STM images obtained at different temperatures. The image taken at 150 K (Figure 4a) reflects the situation as shown in Figure 3. This wide-range scan shows that the filaments are formed more via alkyl chain interdigitation than via backbone−backbone interactions. At 200 K (Figure 4b), homochiral molecular lines grow into an elongated 2D pattern. Inside the molecular islands, the parallel bright rows can be easily interpreted as molecular backbones and the dim stripes between the bright rows are the alkyl chains. The growth is asymmetric, indicating that the self-assembly via interdigitation of the alkyl

(46) Lingenfelder, M.; Tomba, G.; Costantini, G.; Ciacchi, L. C.; De Vita, A.; Kern, K. *Angew. Chem., Int. Ed.* **2007**, *46*(24), 4492.

(47) Chen, Q.; Frankel, D. J.; Richardson, N. V. *Langmuir* **2002**, *18*, 3219.

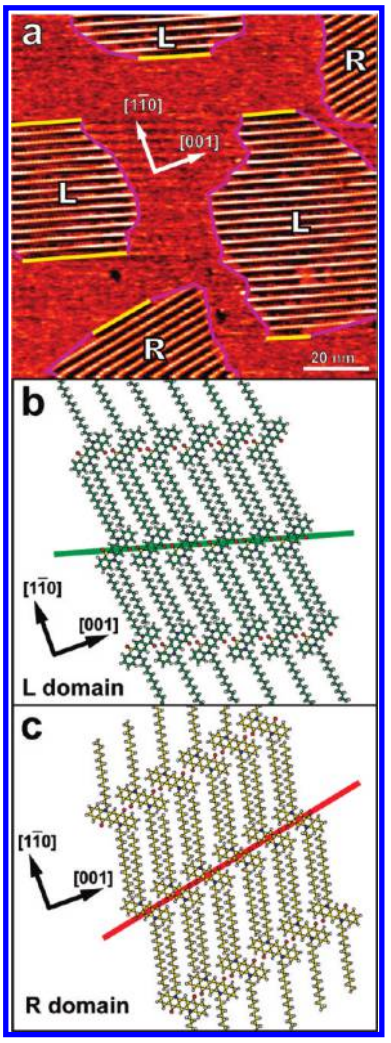

Figure 5. (a) Large-scale STM image ($U_{bias} = -1.01$ V, and $I_t = 0.78$ nA) of QA16C on Cu(110) acquired at room temperature. Two mirror domains (L and R) are observed. Yellow solid lines indicate straight domain boundaries, while pink curves represent boundaries with higher kink density. (b and c) Models for L- and R-domains showing the orientation of the backbone lines as observed in panel a.

chains occurs faster at that temperature. In addition, it shows that homochiral recognition goes not only along the backbone line but also via the interdigitation. This can be understood by steric constraints; i.e., good interdigitation is achieved only with an identical backbone orientation. Consequently, only two types of domains, L- and R-domains, are observed.[48] This contrasts with earlier work with similar molecules on HOPG, where a small change in chain length had an influence on the optical resolution.[49] Further increasing the sample temperature to 250 K leads to fewer but larger molecular islands (Figure 4c). Additional features, like dim spots, observed between the islands are probably caused by molecules that have been picked up by the tip, rather than isolated stationary molecules. With enhanced surface diffusion, more molecules become incorporated into the islands. This trend continues to 300 K where even larger parallel-line domains are observed (Figure 4d). We note that no desorption or decomposition of molecules is expected below room temperature.

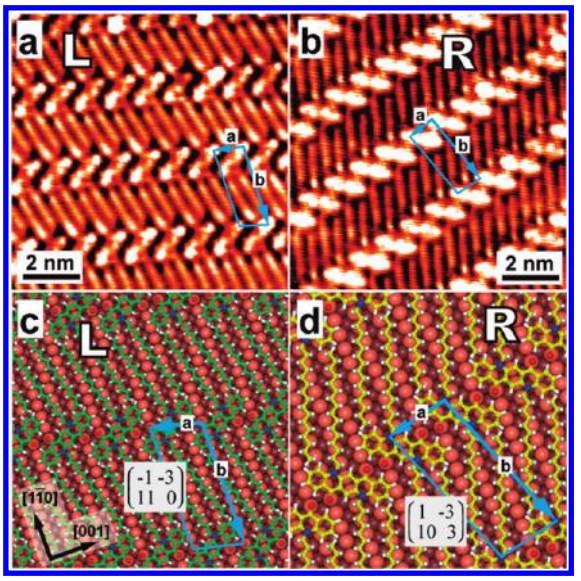

Figure 6. (a and b) High-resolution STM images at 300 K [(a) $U_{bias} = -1.05$ V, and $I_t = 0.80$ nA; (b) $U_{bias} = -1.00$ V, and $I_t = 0.80$ nA] of the two mirror domains formed by QA16C on Cu(110). Aromatic backbones and alkyl chains of the molecules are well-resolved. Unit cells are colored blue. (c and d) Models for the L- and R-domain structures, aligned with respect to the corresponding STM images in panels a and b.

There are different shapes observed for the domain boundaries, depending on whether they are terminated by alkyl chains or the ends of the backbone lines. This is shown in the large-scale STM image recorded at 300 K (Figure 5a). Every island has two smooth boundaries and two rough boundaries, marked by yellow and pink lines, respectively. The straight boundaries coincide with the bright backbone lines, while the alkyl chains of these straight boundary molecules pointing away from the island are not resolved. Assuming an attachment−detachment equilibrium of the 2D crystal phase and the 2D gas phase, a straight boundary suggests that the intermolecular forces along the backbone lines (indicated by green and red solid lines in Figure 5b,c) are substantial. Therefore, the barrier to create a kink here is higher. A higher kink density is observed at the boundaries running perpendicular to the bright backbone lines and implies a higher growth rate. This explains that the island shape at this temperature is no longer so elongated.

With increasing coverage, the L- and R-domains become larger, until the whole surface is covered. Except for these two enantiomorphs, no different crystal phases have been observed at different coverages and temperatures. High-resolution STM images recorded at 300 K are shown in Figure 6. The backbones and alkyl chains are well-resolved, showing that the latter are interdigitated in a parallel arrangement. This motif has often been observed on HOPG and installs additional intermolecular interactions via van der Waals forces. The length of alkyl chains in the domains is uniformly 1.9 nm, which equals the value of a straight chain in vacuum. Thus, the chains lie flat and extend freely on the substrate. No matter which domain, the angle between the alkyl chains and the long axis of the backbone is 102°. This angle results from the parallel arrangement of the alkyl chains, which is favored over other distributions at this temperature. The 2×2 transformation matrices for these lattices are (−1 −3, 11 0) and (1 −3, 10 3).[50] This gives an area of the unit cell of this superstructure of

(48) The C_2 symmetry of the substrate makes rotational domains of these structures indistinguishable.

(49) Wei, Y.; Kannapan, K.; Flynn, G. W.; Zimmt, M. B. *J. Am. Chem. Soc.* **2004**, *126*, 5318.

(50) ($\mathbf{m_{11}}$ $\mathbf{m_{12}}$, $\mathbf{m_{21}}$ $\mathbf{m_{22}}$) links the adsorbate lattice vectors ($\mathbf{b_1}$, $\mathbf{b_2}$) to the substrate lattice vectors ($\mathbf{a_1}$, $\mathbf{a_2}$) via $\mathbf{b_1} = \mathbf{m_{11}a_1} + \mathbf{m_{12}a_2}$ and $\mathbf{b_2} = \mathbf{m_{21}a_1} + \mathbf{m_{22}a_2}$: Park, R. L.; Madden, H. H. *Surf. Sci.* **1968**, *11*, 188.

3.05 nm^2 and corresponds to 33 Cu surface atoms. Figure 6 also shows structural models for both enantiomorphs that are in agreement with the STM observations. We tentatively placed each oxygen atom of the QA16C molecule on top of a copper atom. This adsorption configuration has been identified for QA16C on Ag(110) by density functional theory (DFT) calculations.[34] The formation of a line by aromatic backbones at low coverage must be attributed to attractive intermolecular interactions, most probably hydrogen bonds between the oxygen atoms and hydrogen atoms at the adjacent aromatic backbones.

Interestingly, there is no phase transition with increasing coverage. From one-dimensional (1D) molecular lines to 2D extended molecular islands, the backbone of a single QA16C enantiomer keeps one uniform orientation on the Cu(110), no matter the temperature or coverage. This suggests quite strong interactions between the molecules and the substrate. A binding energy of −1.54 eV has been calculated by DFT for QA1C, i.e., basically the backbone only, on Ag(110).[34] For copper, an even stronger binding of the backbone must be expected. A denser heterochiral structure on Ag(110) has been observed for the QA4C derivative, which has substantially shorter alkyl chains.[34] To induce a denser packing of the backbones, the alkyl chains of QA16C are required to be lifted away from the surface, as sometimes observed for the HOPG/liquid systems.[51] However, the energy of binding of the alkyl chains to the Cu(110) surface represents a barrier that is too high to allow higher coverages. Consequently, the system stays homochiral and does not allow a chiral phase transition into a racemic 2D crystal, as observed previously for other systems.[52−54] Although intermolecular interactions such as van der Waals forces between the alkyl chains and hydrogen bonding between the aromatic cores are at work here, the enantioselectivity is primarily based on the alignment of the molecule by the substrate.

Conclusions

Real-space observations with the STM provide valuable insight into mechanism of molecular recognition at surfaces. We have shown here that the strict alignment of a long alkyl chain quinacridone derivative on a surface has consequences with respect to the optical resolution of enantiomers. This alignment, in connection with the steric influence of the long alkyl chains, strongly favors homochiral recognition. This results in a 2D conglomerate at all coverages. Beyond this molecule−substrate mechanism, intermolecular forces such as hydrogen bonding between the aromatic backbones and van der Waals interactions between the alkyl chains contribute to the transfer of chirality from the single molecule via 1D molecular lines into 2D domains.

Acknowledgment. This work was supported by NSFC (Grants 10674159 and 10874219), Projects '863'and '973' in China. K.-H.E. thanks the Swiss National Science Foundation (SNSF) for support.

(51) De Feyter, S.; Larsson, M.; Gesquire, A.; Verheyen, H.; Louwet, F.; Groenendaal, B.; van Esch, J.; Feringa, B. L.; De Schryver, F. *Chem. Phys. Chem.* **2002**, *11*, 966.
(52) Romer, S.; Behzadi, B.; Fasel, R.; Ernst, K. H. *Chem.—Eur. J.* **2005**, *11*, 4149.
(53) Vidal, F.; Delvigne, E.; Stepanow, S.; Lin, N.; Barth, J. V.; Kern, K. *J. Am. Chem. Soc.* **2005**, *127*, 10101.
(54) Böhringer, M.; Schneider, W. D.; Berndt, R. *Angew. Chem., Int. Ed.* **2000**, *39*, 792.